Jb. Geol. B.-A.	ISSN 0016-7800	Band 133	Heft 4	S. 549–560	Wien, Dezember 1990

Analysis of Kinematics in Faulted Rocks: A Methodical Comparison with an Example from the Eastern Alps (Austria)

By HARALD FRITZ, FRANK SCHRADER & ECKART WALLBRECHER*)

With 10 Figures and 1 Table

Austria
Eastern Alps
Fault analysis
Methodical approach
Stress
Displacement
Gröden Sandstone

Österreichische Karte 1 : 50.000
Blatt 197

Contents

Zusammenfassung

Für einen Vergleich zweier neuer Methoden zur Harnischanalyse wurde ein Aufschluß nach diesen Verfahren untersucht und die Ergebnisse wurden mit denen nach der Methode von ANGELIER & MECHLER (1977) verglichen. Gemeinsam ist beiden Verfahren (im Gegensatz zu vielen anderen), daß die Information aus möglichst vielen verschieden orientierten Harnischen und nicht aus deren Verteilungshäufigkeit gewonnen wird.

Nach der Versetzungsfeld-Methode von SCHRADER (1987, 1988b) wird im Aufschluß gezielt nach verschiedenen Richtungen gesucht und gleichzeitig manuell ausgewertet. Dadurch sind vergleichsweise wenige Harnische zur Analyse erforderlich. Das Ergebnis wird sofort ermittelt als Feld deformativer Versetzungen. Seine Richtungen (Einengung und Dehnung) und seine Deformationssymmetrie (Zweischarige Scherung, etc.) können erkannt werden.

Nach der Orientierungs-Tensor Methode von WALLBRECHER & FRITZ (1989) werden größere Datenmengen numerisch verarbeitet: Für unterschiedliche Formfaktoren des deviatorischen Spannungsellipsoids (σ_1-, σ_2-, σ_3-Verhältnisse) wurden auf hypothetischen Harnischflächen die resultierenden Harnischstriemungen berechnet. Der Orientierungstensor von natürlichen Striemungen wird mit den Orientierungstensoren der theoretischen Striemungen verglichen und so die Orientierung und die Proportionen der Hauptachsen σ_1, σ_2, σ_3 des deviatorischen Stressellipsoids quantitativ ermittelt.

Beide neuen Methoden liefern ähnliche Ergebnisse wie das Analyseverfahren nach ANGELIER & MECHLER (1977). Vorteile, Ausdruckskraft und Anwendbarkeit der Methoden werden diskutiert.

Abstract

To test two new methods of fault-analysis we examined one outcrop in the Gail valley and compared the results with those according to the fault analysis method of rectangular dihedra of ANGELIER & MECHLER (1977). Both new methods use data from faults of as many different orientations as possible and not from distribution density like other methods do.

According to the displacement field method of SCHRADER (1987, 1988b) the outcrop is searched selectively for different fault-orientations which are analysed manually at the same time. Only a comparably small number of faults is necessary.

*) Authors' addresses: Dr. HARALD FRITZ, Univ.-Prof. Dr. ECKART WALLBRECHER, Institut für Geologie und Paläontologie, Universität Graz, Heinrichstrasse 26, A-8010 Graz; Dr. FRANK SCHRADER, Geologisches Institut der Universität Bonn, Nußallee 8, D-53 Bonn 1; present address: c/o Department of Geology, Earth Sciences Centre, University of Toronto, 22 Russell Street, Toronto M5S 3B1, Ontario, Canada.

The result is got at once as a field of deformational displacements. Its directions (compression and extension) and its deformation symmetry (pure shear, etc.) can be recognized.

Using the orientation tensor method after WALLBRECHER & FRITZ (1989) larger data-quantities are analysed numerically. Theoretical striation pattern were calculated for systematically variing shape factors of the stress ellipsoid. The orientations and proportions of the axes σ_1, σ_2, σ_3 of the deviatoric stress ellipsoid are determined quantitatively by comparing natural field data with these theoretical striation pattern.

All three methods give similar results. Expressiveness, advantages and applicability of the methods are weighted.

1. Introduction

Joints and faults are very important tectonical structures in the upper crust, where rocks have reacted to stresses by brittle material behaviour. Faults, which are fractures on which displacements have taken place, are used for kinematic analysis in brittly deformed rocks.

Experimental studies show that certain stresses cause sets of faults in preferred orientations (e.g. v. KARMAN, 1911; PRICE, 1966; MANDL, 1988). Based on this phenomenon, methods were evolved to determine the orientation of principal stresses (e.g. ANDERSON, 1952). But faults also occur in other orientations, and ARTHAUD (1969) established a method to analyse them collectively as an (initial) ellipsoid of finite strain XYZ.

BOTT (1959) postulated that slip-striations on fault planes develop parallel to the direction of MRSS (Maximum Resolved Shear-Stress) of a stress-field acting along these planes. He calculated the MRSS on arbitrarily oriented planes in relationship to the ratio of the values of principal stress axes. Many methods to analyse faults as stresses were based on this concept (e.g. ANGELIER & MECHLER, 1977; ALEXANDROWSKI, 1985). Various computer applications were published by CAREY & BRUNIER (1974), CAREY (1976, 1979), ARMIJO & CISTERNAS (1978), ANGELIER & GOGUEL (1979), ANGELIER & MANOUSIS (1980), and PFIFFNER & BURKHARD (1987). ETCHECOPAR et al. (1981) and ARMIJO et al. (1982) calculated the stress tensor directions from slickenside striations. SIMON GOMES (1986) and DE VICENTE (1988) also followed BOTT's concept but extended his formula further to calculate stress proportions in naturally deformed rocks.

Whereas preferredly oriented major fault planes are helpful for the estimation of stress directions, randomly oriented minor faults are useful for the exact determination of orientation and shape of the stress ellipsoid. WALLBRECHER & FRITZ (1989) calculated the MRSS (Maximum Resolved Shear-Stress) on homogeneously distributed planes for systematically variing proportions of principal stresses. The orientation distribution of MRSS-directions which, according to BOTT, coincide with slip-striations, is characterized by its orientation tensor. The results of these theoretical considerations are used to calculate shape and orientation of the stress-ellipsoid in natural rocks.

Slip lineations are not only visible on fault planes, but also on pebbles in conglomerates, which were de-

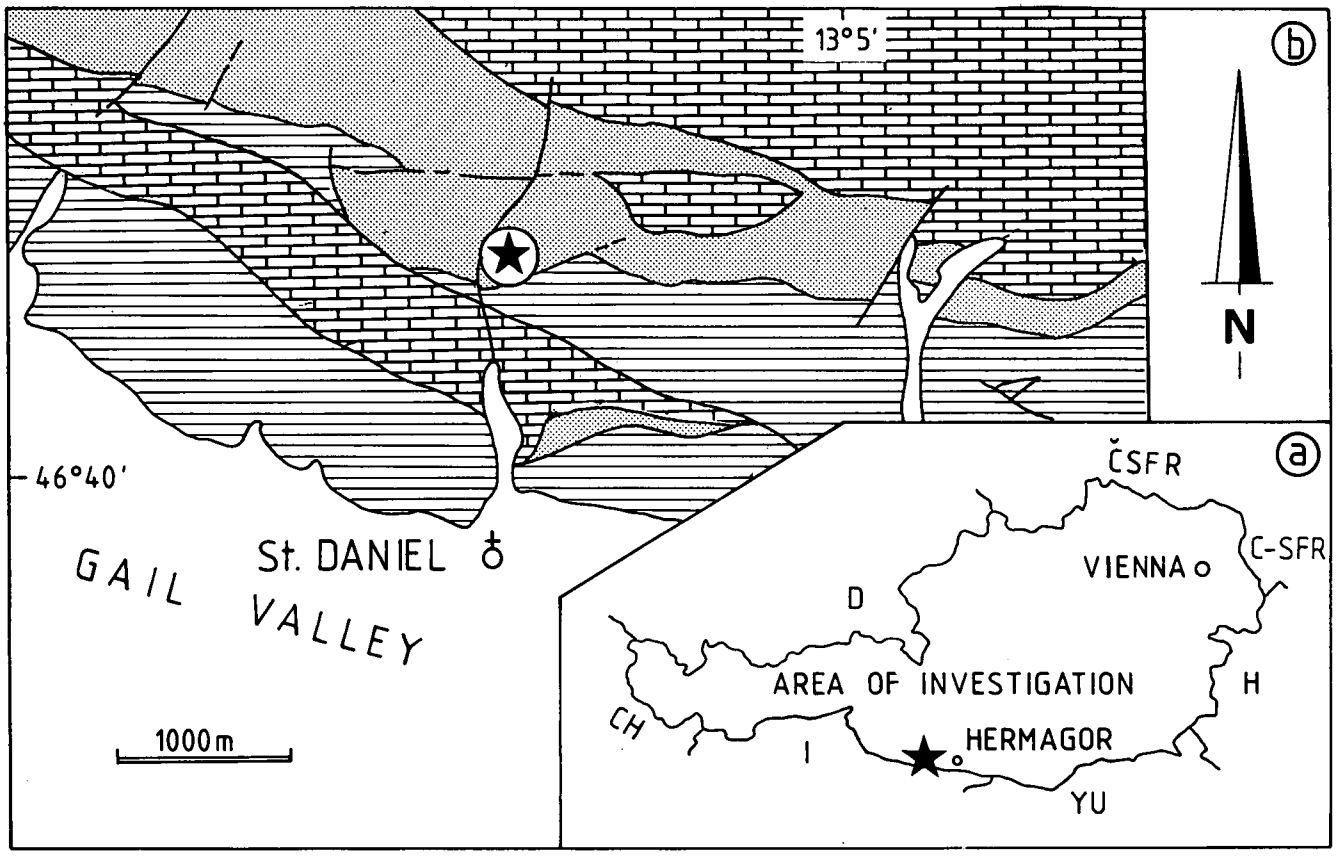

Fig. 1.
a) Location of the examined outcrop (forest path near St. Daniel, west of Hermagor/Kärnten).
b) Geological map, simplified after SCHÖNLAUB (1985).
Line ornament = Gailtal crystalline (undifferentiated); stippled = Permotriassic clastics of the Drauzug with the locality of investigation (•); wall signature = Triassic limestones of Drauzug.

formed by relative displacements of the individual pebbles (SCHRADER, 1988a). Pebble surfaces can be considered as an infinite number of tangent planes to a sphere and define displacement planes of all directions. Following this idea SCHRADER (1988b) represented all the slip directions on the fault planes found in an outcrop in an equal area plot. From the pattern of these lineations the geometry of the field of slip-lineations is deduced.

So SCHRADER and WALLBRECHER & FRITZ came, first following different ideas, to similar considerations. Slickenside striation analysis is done with fault planes of as many directions as possible. Not only the major faults following the COULOMB behaviour of preferred orientation, but also the minor faults in ancilliary orientation provide the best information for kinematic analyses.

2. Regional Setting and Phenomenon

To compare the different methods we examined a faulted rock in massive Gröden Sandstone, which is the basal formation of the „Drauzug" unit of the Upper Austroalpine nappe pile (Fig. 1). Although there is evidence of a primary sedimentary contact between Drauzug and the underlying Gailtal crystalline, the present contact is mostly tectonic, as seen in the map scale structures (SCHÖNLAUB, 1979, 1985, 1987; VAN BEMMELEN, 1961; HEINISCH et al., 1984; HEINISCH, 1988). Both, the Gailtal crystalline and the basal Drauzug suffered left lateral shear deformation in Alpidic time; progressive brittle conditions towards the Drauzug are evident from microstructures (UNZOG, 1988). Dextral structures (e.g. the Periadriatic lineament) finally crosscut the sinistral structures and complicate the structural pattern.

In the analysed outcrop the Gröden beds occur as sandstones with some pebbles. The massive sandstones are intensely faulted. The sense of displacement on each fault is recognized by stepwise growth of fibre minerals (Fig. 2).

3. Methodical Procedures

In the following a short introduction to the methodical procedures is given; for a detailed description the reader is referred to the literature (ANGELIER & MECHLER, 1977; SCHRADER, 1987, 1988b; WALLBRECHER & FRITZ, 1989).

3.1. The Displacement Field Method after SCHRADER

This concept is based on the observation of slip lineations and solution pits on the surfaces of non-ductilly deformed pebbles from the northern Alpine Molasse zone (SCHRADER 1988c). The same features can also be seen on pebbles from the Gröden sandstone we found close to the outcrop of our fault-example. The slip directions on a homogeneously distributed set of fault planes show a similar displacement pattern.

In the SCHMIDT net, a displacement direction is recorded by the pole of the plane and the slickenside striation. A small arrow through the pole of the plane parallel to the great circle, which contains also the point of penetration of the striation linear (with the arrowhead pointing into the relative slip direction), represents the fault (HOEPPENER, 1955; Fig. 3). The faults in an outcrop are measured and recorded subsequently until the fault-arrows cover all domains of the SCHMIDT net. In order to find as many orientations as possible, each fault is recorded after measurement, and faults in the directions still missing in the diagram are then searched.

The usual displacement field has a triaxial geometry (Fig. 4a; SCHADER, 1988a) which is made visible in the diagram by interpolation with lines of course parallel to the single fault arrows of similar direction and sense of displacement (Fig. 5). Displacement lines diverge from the axis of divergence (AD), change their directions at the intermediate axis (AI) and converge to the axis of convergence (AC). The plane of divergence (PD) comprises AD and AI and the plane of convergence (PC) comprises AI and AC. It is worth noting that axes and

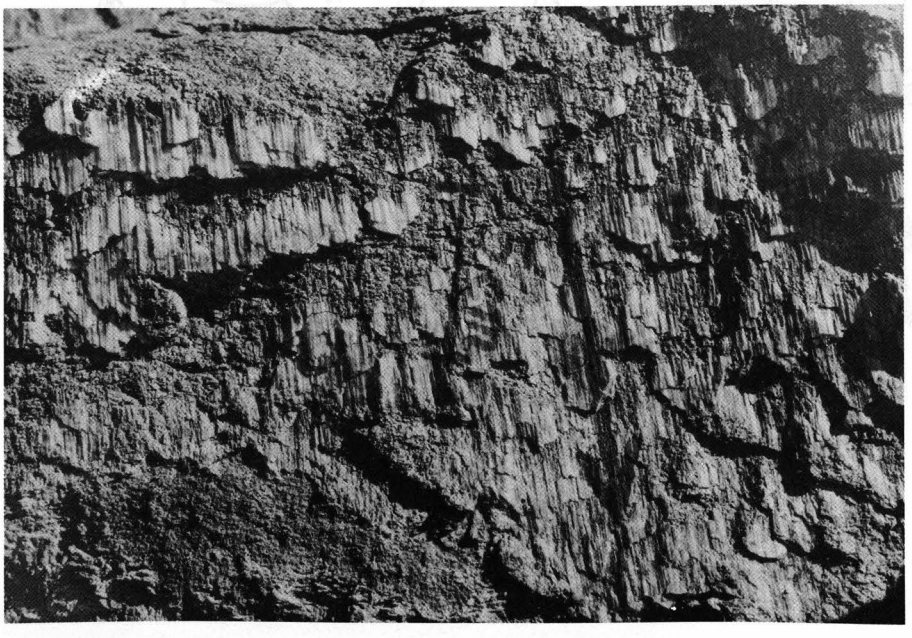

Fig. 2.
Typical fault in the Gröden sandstone.
The displacement sense of slickenside striations (arrow direction) is recognized by crystal fibre growth with steps pointing in direction of relative displacement (congruous, NORRIS & BARRON, 1968).

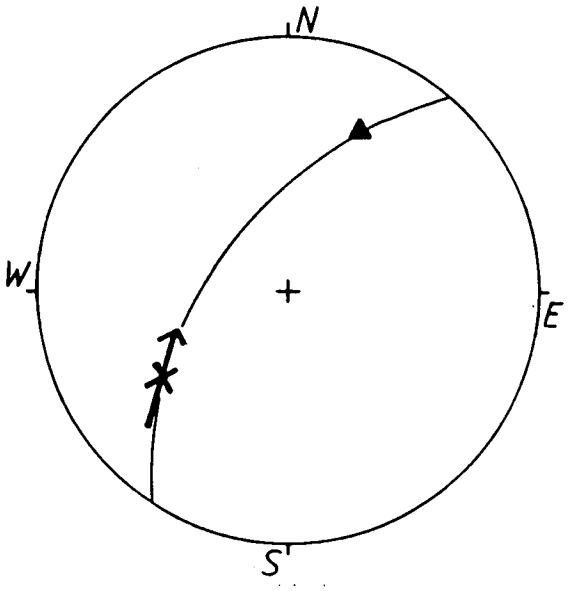

Fig. 3.
Technique of fault representation (according to HOEPPENER, 1955; used in the method of SCHRADER).
At the pole of the fault plane (x), a fault-arrow —x→ is plotted parallel to the great circle towards the penetration point of the striation (▲). The movement direction is indicated by an arrowhead pointing into the displacement direction of the lower block. The lower hemisphere equal area projection is used in this paper for better comparison of the diagrams of the different methods. The use of the upper hemisphere projection is more suitable in practice when the rock is searched for faults in all directions.

planes may show an orthogonal arrangement, but need not.

The arrangements are congruent with the movement patterns of particle motion fields as calculated by HOEPPENER (1964) and RAMBERG (1975) and thus are interpreted to represent them. AD is the direction of approaching particles (compression); AC is the direction in which the particles move away from each other (extension). Orthogonal, triaxial cases represent the deformation symmetry of pure shear (Fig. 4). In this case, AD corresponds with σ_1 (stress) and Z (finite strain) ; AC with σ_3 and X; and AI with σ_2 and Y. If AI and AC are not differenciated along PC (no bending of dis-

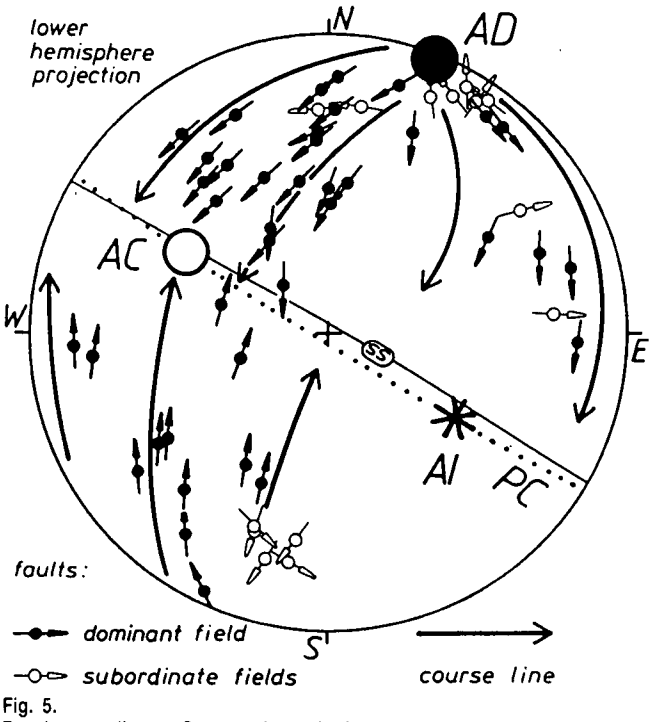

Fig. 5.
Result according to SCHRADER's method.
The displacement field is interpolated by lines of course between individual arrows. A dominant field with clear AD perpendicular to PC is associated with faults of differing subordinate fields. The symmetry of the dominant field is close to uniaxial compression, in the range towards pure shear (Fig. 4), because the differentiation of PC to AI and AC is only slight.

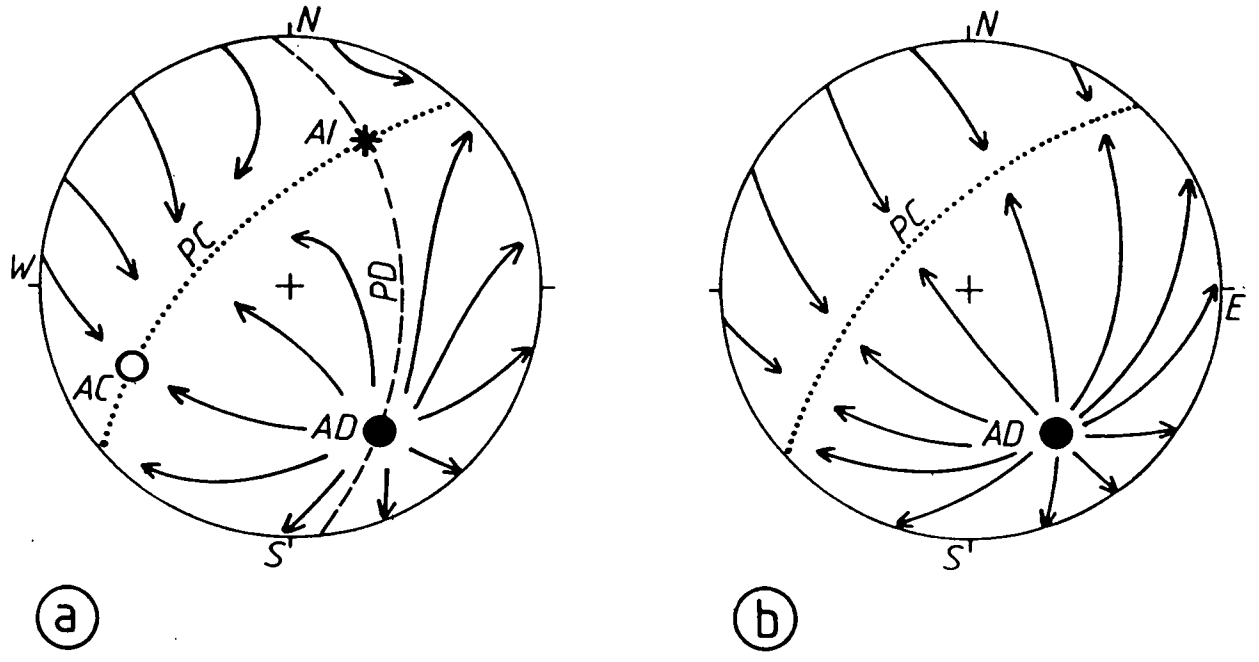

Fig. 4.
Displacement field.
The displacements are indicated by lines of course → parallel to fault-arrows (Figs. 3, 5). They change directions at axes (AD•, AI ⋆, AC○) and planes of the displacement field (PD ----, PC ·····; for explanation see text). Their arrangement must not be orthogonal.
a) Triaxial arrangement (pure shear).
b) Uniaxial divergence-arrangement (uniaxial compression); AI and AC are not differenciated along PC.

placement-lines reaching PC, Fig. 4b) and PC is perpendicular to AD, the arrangement has uniaxial divergence symmetry corresponding to uniaxial compression deformation symmetry. Non-orthorhombic arrangements might represent other deformation symmetries (simple shear, etc.; SCHRADER, 1988c).

3.2. The Orientation Distribution Tensor Method of WALLBRECHER & FRITZ

The direction of the Maximum Resolved Shear Stress (MRSS) on a plane depends on the orientation of this plane in respect to the principal stresses and their magnitude relations. BOTT (1959) postulated that slickenside striation develops in the direction of MRSS. WALLBRECHER & FRITZ (1989) used BOTT's formula (equation 1) to model striation patterns for homogeneously oriented, hypothetical fault planes at systematically changing stress proportions $|\sigma_1| : |\sigma_2| : |\sigma_3|$. BOTT's formula

$$\tan \Theta = \frac{n}{lm}\left[m^2 - (1-n^2)\,\frac{\sigma_1 - \sigma_2}{\sigma_2 - \sigma_3}\right] \qquad (1)$$

can be transformed to

$$\tan \Theta = \frac{n}{lm}\left[m^2 - \frac{1 - n^2}{R}\right] \qquad (2)$$

in order to keep the form factor R (equation 3) of the stress ellipsoid in the range of $0 \leq R \leq 1$. The form factor controls the shape of an ellipsoid and is given as:

$$R = (|\sigma_2| - |\sigma_3|)/(|\sigma_1| - |\sigma_3|) \qquad (3)$$

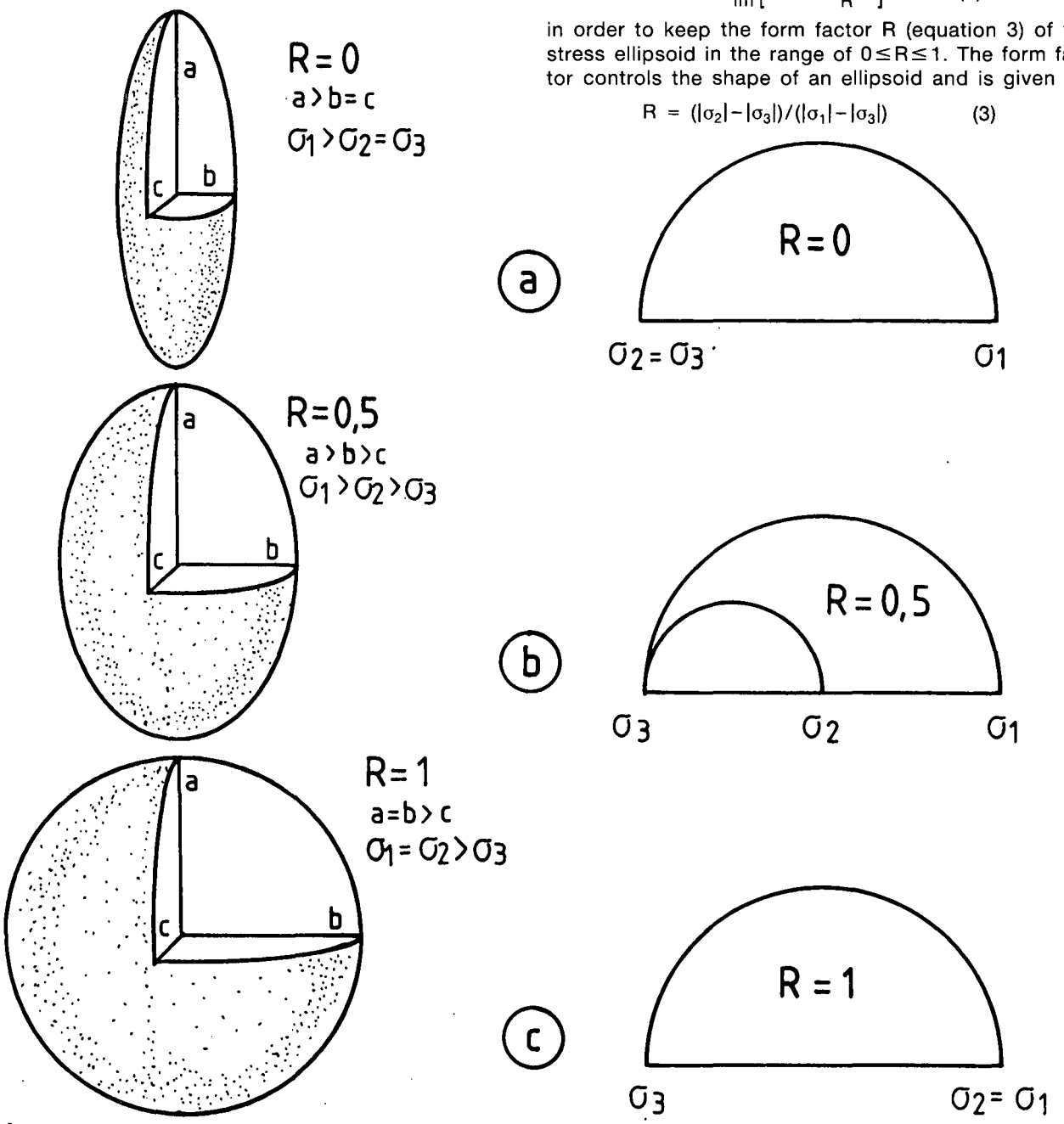

Fig. 6.
The form factor R = (b−c)/(a−c) indicates the shape of an ellipsoid with the axes a,b,c (left).
Corresponding axes of the stress ellipsoid in the formula of BOTT (1959) are $\sigma_1 = a$; $\sigma_2 = b$; $\sigma_3 = c$. The shape can be:
a) Cigar-like ($0 \leq R < 0.5$).
b) Maximum triaxial ($R = 0.5$).
c) Pancake-like ($0.5 < R \leq 1$).
Stress relations can be represented in MOHR circles (right).

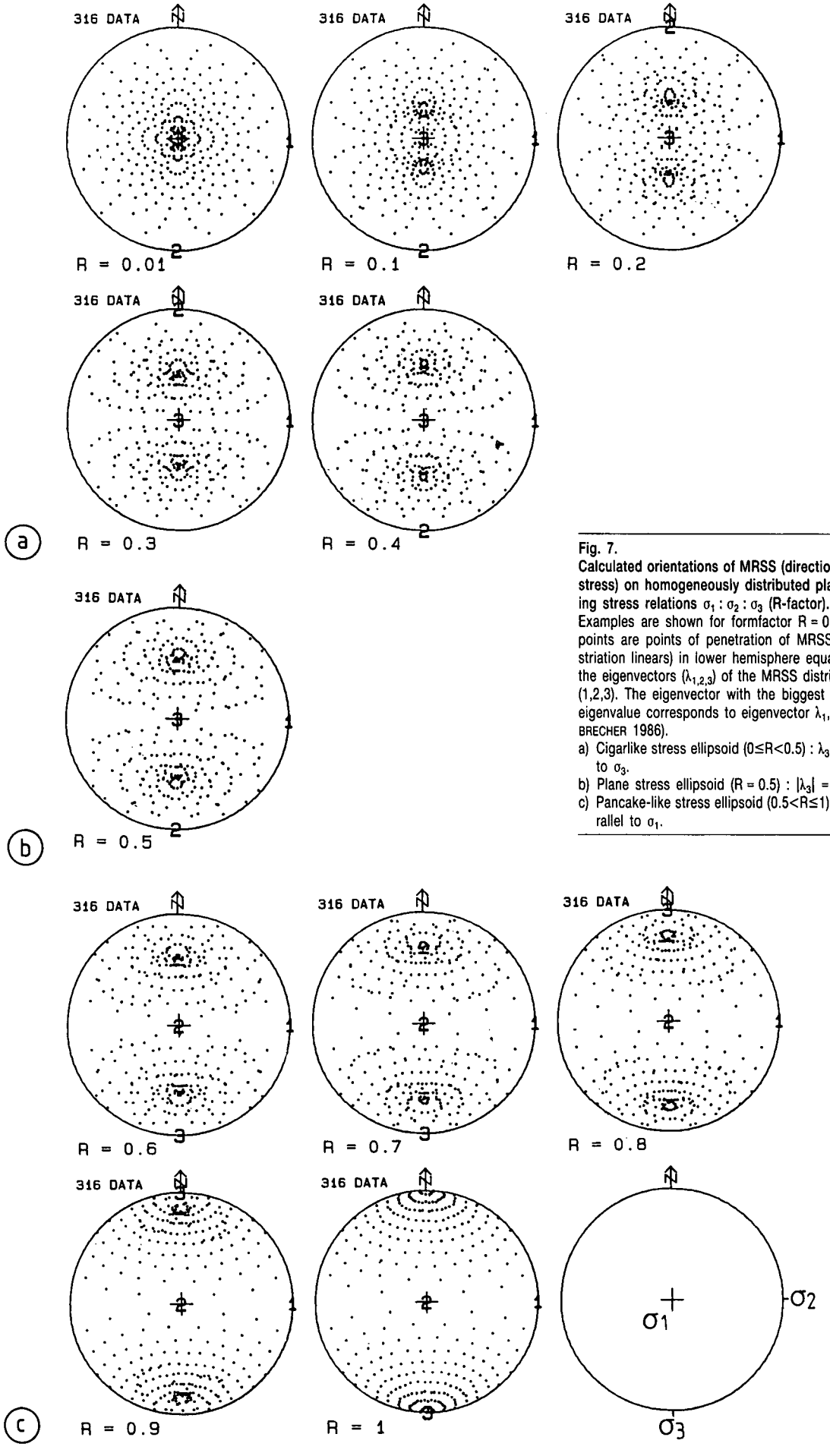

Fig. 7.
Calculated orientations of MRSS (direction of maximum resolved shear stress) on homogeneously distributed planes at systematically changing stress relations $\sigma_1 : \sigma_2 : \sigma_3$ (R-factor).
Examples are shown for formfactor R = 0.01 to R = 1. The represented points are points of penetration of MRSS-linears (taken parallel to the striation linears) in lower hemisphere equal area plots. The positions of the eigenvectors ($\lambda_{1,2,3}$) of the MRSS distribution are shown by numbers (1,2,3). The eigenvector with the biggest eigenvalue is λ_3, the smallest eigenvalue corresponds to eigenvector λ_1, which is parallel to σ_2 (WALLBRECHER 1986).
a) Cigarlike stress ellipsoid ($0 \leq R < 0.5$) : λ_3 is parallel to σ_1 and λ_2 parallel to σ_3.
b) Plane stress ellipsoid ($R = 0.5$) : $|\lambda_3| = |\lambda_2|$.
c) Pancake-like stress ellipsoid ($0.5 < R \leq 1$) : λ_3 is parallel to σ_3 and λ_2 parallel to σ_1.

Θ is the angle of "pitch" between the direction of strike and the striation. l, m, and n are the direction cosines of the normal to the plane as related to a Cartesian coordinate system parallel to principal stresses σ_1, σ_2, σ_3 with σ_1 in a vertical position and σ_3 N–S.

In a set of homogeneously distributed planes, the form factor R (which describes the shape of the stress ellipsoid, Fig. 6) is the only parameter which controls the orientation pattern of MRSS on these planes (Fig. 7). Thus, striation distributions can be correlated with the shape (R-factor) of the stress ellipsoid. To avoid misinterpretations by the visual interpretation of confusing point representation patterns, the distribution of striations is expressed numerically by the eigenvalues and eigenvectors of their orientation tensor (WALLBRECHER, 1986). This procedure is carried out by a computer program which gives the eigenvalues and eigenvectors of any orientation data as well as a value for the degree of orientation preference in R-% (WALLBRECHER, 1986), which indicates how homogeneously the fault- planes of a data-set are distributed.

Results of this model calculation are:

1) The eigenvectors ($\lambda_{1,2,3}$) of the orientation tensor of MRSS are parallel to principal stresses with the smallest eigenvector λ_1 ($|\lambda_1| < |\lambda_2| < |\lambda_3|$) parallel to σ_2. The correlation of λ_2 and λ_3 to σ_1 and σ_3 depends on the shape of the stress ellipsoid. We can distinguish three cases (Fig. 7):
   a) $0.0 \leq R < 0.5$ with λ_2 parallel σ_3 and λ_3 parallel σ_1.
   b) $R = 0.5$ ($|\lambda_2| = |\lambda_3|$).
   c) $0.5 < R \leq 1.0$ with λ_2 parallel σ_1 and λ_3 parallel σ_3.
2) The eigenvalues of these orientation tensors are related to the form factor of the stress ellipsoid (R) in a linear way (Fig. 8). This relation has the form:

$$R = 0.5 + \lambda_2 - \lambda_3 \qquad (4)$$

if σ_1 is parallel λ_3 and σ_3 is parallel λ_2 (Fig. 7a), resp., or

$$R = 0.5 + \lambda_3 - \lambda_2 \qquad (5)$$

if σ_1 is parallel λ_2 and σ_3 is parallel λ_3 (Fig. 7c).

To decide which of both λ_2 or λ_3 of the data set corresponds to σ_1 or σ_3, the displacement sense of single faults can be used; only a few must be known. Displacement is directed (qualitatively) from σ_1 towards σ_3. Numerically, it can be determined by the method of rectangular dihedra (ANGELIER & MECHLER, 1977; Fig. 10).

R = 0 indicates uniaxial compressive stress, which is a cigar-like form of the stress ellipsoid $\sigma_1 > \sigma_2 = \sigma_3$

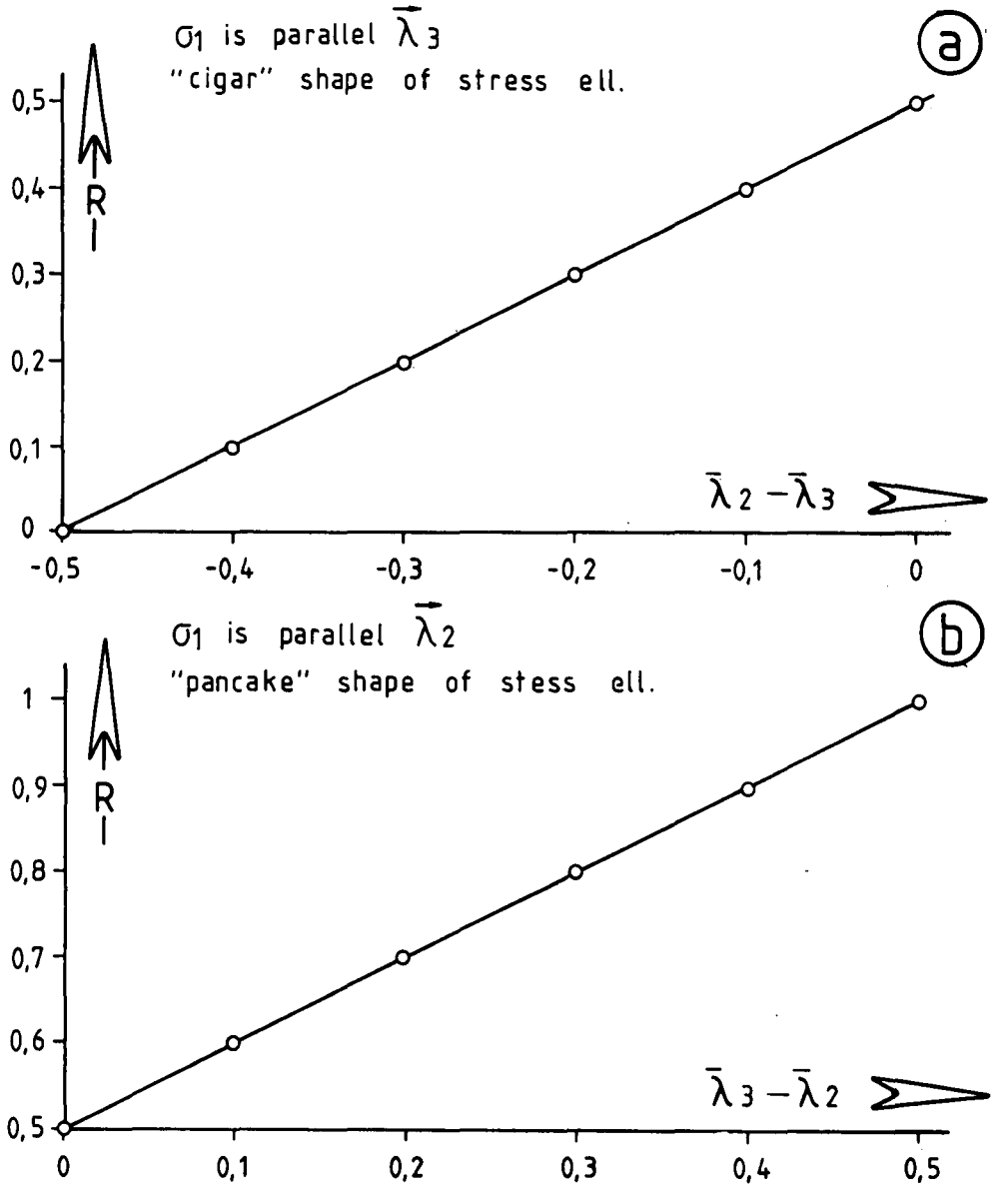

Fig. 8.
Eigenvalues of the orientation tensors of the MRSS direction pattern (horizontal bars) and R-values of the stress ellipsoid (vertical bars) show linear relationships.
Three cases can be distinguished.
a) σ_1 is parallel λ_3 which represents cigarlike shape of the stress ellipsoid and
b) σ_1 is parallel λ_2 which means pancake shape.
At maximum triaxiality of the stress ellipsoid λ_2 and λ_3 have the same value ($|\lambda_3| - |\lambda_2| = 0$), see also Fig. 7. For calculation of R, the eigenvectors λ_2 and λ_3 are assigned to σ_1 or σ_3, respectively, by the fact that displacement is directed qualitatively from σ_1 towards σ_3.

(Fig. 6a); R = 0.5 indicates maximum triaxiality of $\sigma_1 > \sigma_2 > \sigma_3$ (Fig. 6b); R = 1 indicates uniaxial tensile stress, which is a pancake form of the stress ellipsoid $\sigma_1 = \sigma_2 > \sigma_3$ (Fig. 6c). A cigar-like shape of stress is related to flattening strain and a displacement field of uniaxial compression symmetry (Fig. 4b) ; vice versa a pancake shape of stress is related to uniaxially extending displacement symmetry.

The lowest eigenvalue ($|\lambda_1|$) of the MRSS-distribution has been found empirically to be constantly 0.16.

Thus the procedure is as follows: Faults and corresponding slickenside striations are recorded, as many as possible, but only few displacement directions on some faults must be known. If the original fault plane data set does not show the required homogeneous distribution, clustering fault plane poles are eliminated. This procedure is justified because in a uniphase stress field equally orientated planes should get equally orientated striations. By calculating eigenvalues and eigenvectors ($|\lambda_{1,2,3}|$ resp. $\lambda_{1,2,3}$) of the striation pattern corresponding to the uniformly distributed, "cleaned" fault plane data the stress tensor is determinated.

3.3. The Method of Rectangular Dihedra (Angelier & Mechler, 1977)

For each single fault two compressional dihedra and two extensional dihedra are defined. In a Schmidt net the set of dihedra (compressional and extensional dihedra) is constructed using the trace of the fault plane and the trace of a hypothetical plane with the penetration point of the slickenside striation as pole to this plane. For a population of fault measurements the maxima of accumulated compressional resp. extensional dihedra localize σ_1 resp. σ_3.

3.4. Differences and Difficulties

As alredy mentioned, the new methods give most reliable results if fault planes of many directions are present. Although many preferentially oriented fault planes occur approximately in a position of 30°–45° to σ_1, depending on the angle of internal friction, planes of nearly all orientations can be found in some rocks. However, the incomplete distribution of planes in rocks can be a problem. They induce a certain degree of uncertainty, if they are lacking.

The method of Schrader reduces this problem by searching selectively for planes of further orientation to enlarge the information. By this way the striation pattern (Fig. 5) is sucessively elaborated. The advantage of this method is that there is no time consuming measurement of already analysed plane-orientations. A diagram shows clearly, how much information exists and how precisely analysis can be made.

The method of Wallbrecher & Fritz is an automate one. As many fault planes and corresponding slickenside striations as possible are measured (Fig. 9a,b). Homogeneous distribution of fault planes (Fig. 9c) is obtained by eliminating clustering points, supposing that fault planes of the same orientation have equally oriented striations (in cases in which one deformation process produced the faults). This is done by a computer program written by Wallbrecher. From model calculation we conclude that the eigenvalue $|\lambda_1|$ of the MRSS-distribution remains at the constant value of $|\lambda_1| = 0.16$, even when the formfactor R varies. This makes it possible to check the reliability of the results. A differing value of $|\lambda_1|$ of a striation distribution is interpreted as superpositon of different deformation phases, which can have produced different striations on the same planes.

In the procedure of Schrader, each single fault displacement is kept in sight and so it is possible to con-

Table. 1.
Summary of the results from the three methods:
The orientation of AD, AC, and AI (axis of divergence, convergence, intermediate axis) of the particle displacement field correspond with the orientations of the eigenvectors of the slickenside striations (Fig. 9d) $\lambda_{1,2,3}$ which we correlate with σ_2, σ_3, σ_1, resp.
Similar principal stresses resulted from the method of Angelier & Mechler (1977).
Eigenvalues of the slickenside striations (Fig. 9d) $|\lambda_{1,2,3}|$ were used to calculate the shape of the deviatoric stress ellipsoid (equation 4). Again the deformation symmetries of both new methods are very similar.

	planes (used)	results				symmetry
SCHRADER	52 (38)	AD 021/03	AI 124/48	AC 300/45	PC 212/88	between uniaxial compression and pure shear
WALLBRECHER & FRITZ	176 (94)	eigenvector orientation				R=0,38: triaxial stress-ellipsoid with tendency to cigar-shape
		$\lambda_3 // \sigma_1$ 198/02	$\lambda_1 // \sigma_2$ 107/43	$\lambda_2 // \sigma_3$ 280/46		
		eigenvalue				
		$\lvert\lambda_3\rvert$ 0,47	$\lvert\lambda_1\rvert$ 0,18	$\lvert\lambda_2\rvert$ 0,35		
ANGELIER & MECHLER	99 (77)	σ_1 ≈30/0	σ_2 ≈115/40	σ_3 ≈295/30		

trol whether it fits the dominating striation pattern or not (Fig. 5). Whether a non-fitting fault is considered as an effect of scattering and better neglected, or whether it belongs to a second displacement field, which is vailed by the dominant one, but can be reconstructed by selective searching, is decided by the possibility to get further data. Thus it is possible to recognize superimposed deformation systems and to separate different deformational phases.

4. Testing the Methods

To compare the two methods we analysed an outcrop in Gröden Sandstones with vertical bedding at the base of the Drauzug in the Gail valley (Fig. 1).

a) Results according to the orientation tensor method of WALLBRECHER & FRITZ:
176 fault planes and corresponding striations were measured. The primary fault plane data are, as

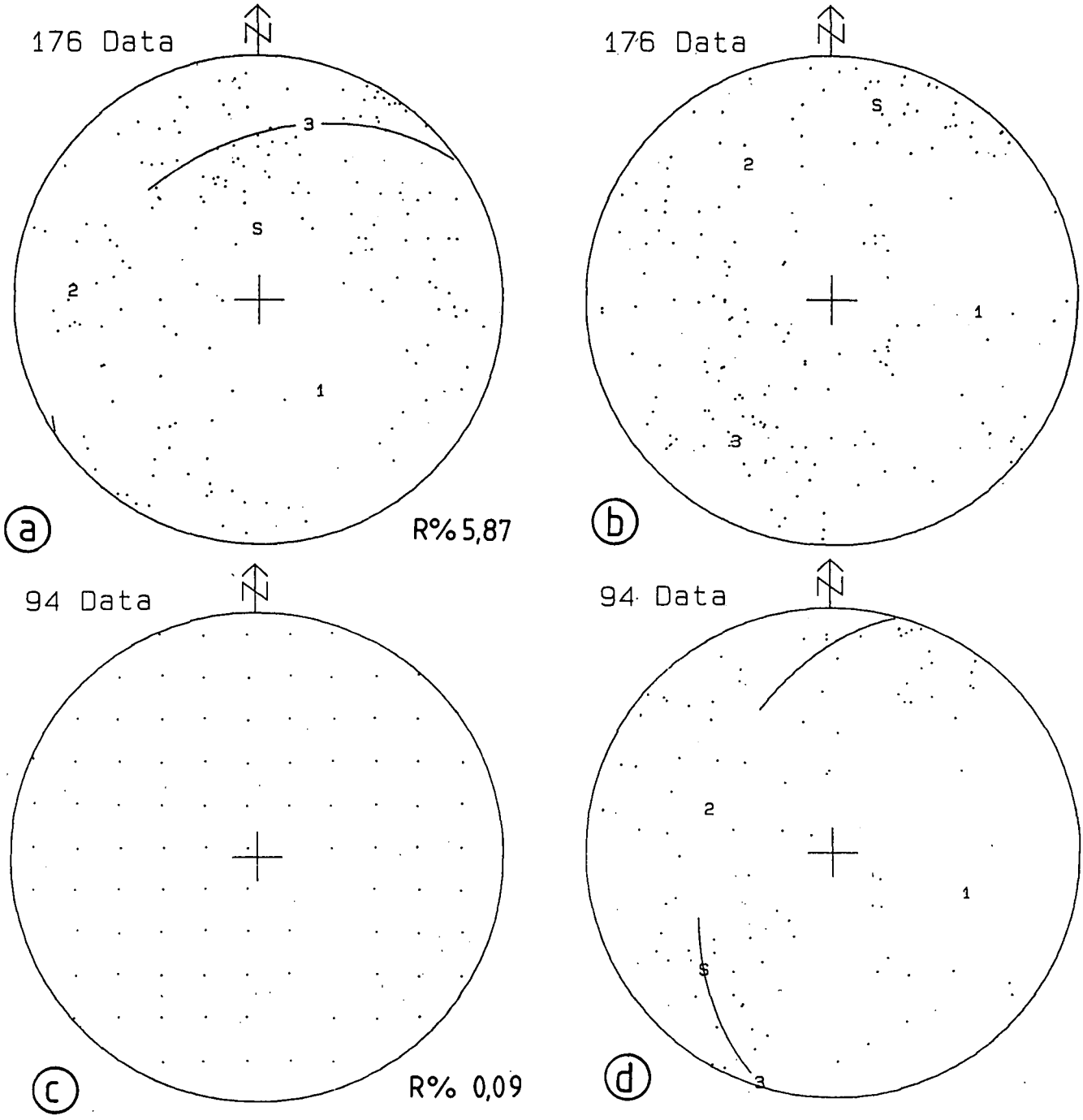

Fig. 9.
The analysing procedure after WALLBRECHER & FRITZ.
a) The original data set consists of fault plane poles (R% is the degree of preferred orientation after WALLBRECHER, 1986) and
b) the corresponding striation linears (points of penetration).
c) Clustering points of the original data set are eliminated (cleaned) by a computer program in order to obtain a nearly homogeneous distribution of plane poles (R% is reduced to 0.09).
d) Finally eigenvectors and eigenvalues of the striations corresponding to the cleaned data set are calculated.
The position of the eigenvectors ($\lambda_{1,2,3}$) in Fig. 9d corresponds to the principal stresses: σ_1 is parallel to λ_3, σ_2 is parallel to λ_1 and σ_3 is parallel to λ_2 (compare with Fig. 10).
The orientations of eigenvectors and eigenvalues are listed in Tab. 1.

usual, not uniformly distributed. Clustering points (Fig. 9a) are eliminated. The cleaned fault planes are nearly homogeneously distributed (Fig. 9c) as seen in the degree of orientation preference which is R% = 0.09 and should be as small as possible. Now we interprete the striations corresponding to the cleaned data (Fig. 9d, Tab. 1).

- The smallest eigenvalue (of the eigenvector λ_1, orientation 107/43) of the striation pattern, which is parallel to σ_2, has the absolute size $|\lambda_1| = 0.18$ which is very close to the theoretical value of $|\lambda_1| = 0.16$ of an ideal MRSS distribution. Therefore we conclude that one deformational phase is responsible for the striation pattern.

- For the interpretation of λ_2 (orientation 280/46) and λ_3 (orientation 198/02) as σ_1 or σ_3, resp., we compare their orientations with the results of the method of ANGELIER & MECHLER (1977) applied on the same data set (Fig. 10). The result of SCHRADER's method also enables the interpretation showing that displacement (Fig. 5) must be directed qualitatively from σ_1 towards σ_3. Our λ_3 turns out to be parallel to σ_1 and λ_2 parallel to σ_3. Table 1 sumarizes the orientations of eigenvectors and their eigenvalues of the striation pattern of the fault planes.

- The form factor R of the stress ellipsoid is 0.38, which results from equation (4)

$$R = 0.5 + \lambda_2 \parallel \sigma_3 - \lambda_3 \parallel \sigma_1$$
$$R = 0.5 + 0.3 - 0.47$$
$$R = 0.38$$

R = 0.38 (Fig. 7) indicates that stress acting in this area is an ellipsoid between cigar-shape (Fig. 6a) and maximum triaxiality (Fig. 6b). Vice versa the corresponding strain geometry is expected between plane strain and flattening strain.

b) Results according to the displacement field method of SCHRADER (Fig. 5):
38 faults were searched selectively in as many directions as possible.

- One system of striations is dominant, but there are one or two others which are vailed by the dominant one.
- The striation pattern clearly shows AD (21/03) and PC (212/88) nearly perpendicular to AD. Along PC, AC (which is the point where striations converge, Fig. 4a) and AI (where displacements bend off) can be only roughly distinguished (AI approximately 124/48, AC approximately 300/45).
- Thus PC is a plane of nearly equal extension in all directions, because AI and AC are nearly of the same nature along PC. The deformation symmetry is more uniaxial compression than pure shear.

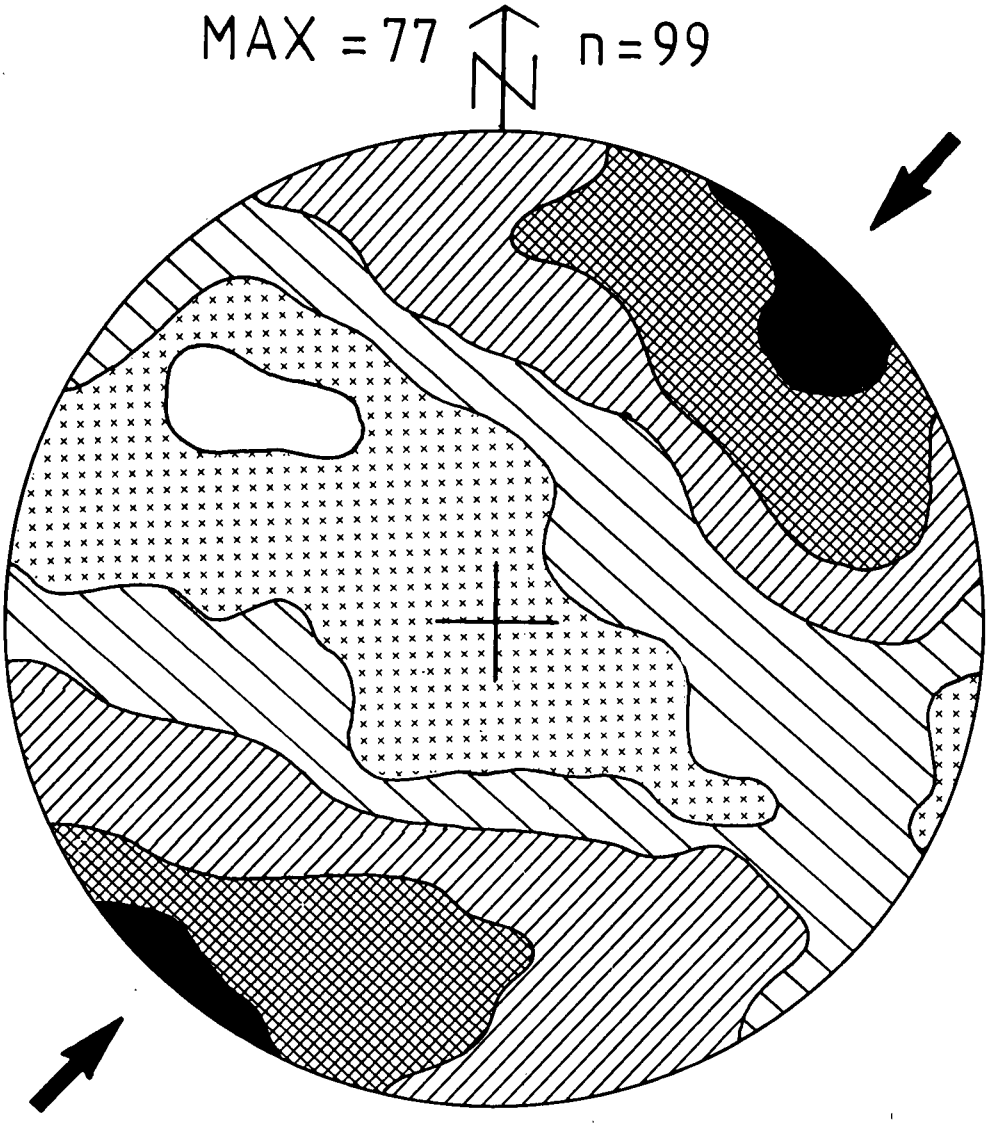

Fig. 10.
Result after the method of ANGELIER & MECHLER (1977).
Fault planes and striations are recorded in spherical projection as "dihedra" and their distribution density is represented by isolines of "superposed compression areas" from 0 % (white) over 25 %, 50 %, 75 % to 100 % (black). σ_1 (arrows) is fixed in the black area and σ_3 in the white area; they have to be mutually perpendicular. n is the number of cumulated dihedra, and MAX is the number of data which are consistant with this solution. Mention that σ_1 and σ_3 correspond to λ_3 and λ_2 of the orientation tensor of Fig. 9.

4.1 Compatibility of the Results

There is a close conformity of the results from the applied methods. The directions of the eigenvectors (Fig. 9d), which are assigned to principal stresses (Fig. 10, Tab. 1), fit well to axes and planes of the displacement field (Fig. 5) and to the results from the method of rectangular dihedra (Fig. 10. Tab. 1). WALLBRECHER & FRITZ calculated a form factor of the stress ellipsoid R = 0.38, which coincides with the determination of the deformation symmetry by SCHRADER between uniaxial compression and pure shear. Further vailed displacement systems are indicated by some deviating arrows in the diagram (Fig. 5). The lowest eigenvalue $\lambda_1 = 0.18$ differs only slightly from the theoretical value of 0.16 for a single phase stress field and thus indicates that deformation was not completely uniphase. It remains to be proven whether the results of the three methods coincide in cases of non-orthogonal displacement-fields.

The results of fault-analysis fit to the results of strain determinations in the ductile structures of the underlying Gailtal crystalline (UNZOG, 1988) . He found an ellipsoid with the long axis parallel to WNW–ESE-direction, discussed it in the context of left-lateral strike-slip-structures combined with a significant flattening component in the ductile Gailtal crystalline and interpreted it as result of NNE–SSW compressive stresses at the base of the brittly deformed Drauzug.

5. Applications

For orthogonal and uniphase fields, the methods give compatible results. However, under some circumstances one or the other should be preferred.

If there is only a small number of faults, but good criteria for the sense of displacement on each of them (Fig. 2), one would use SCHRADER's method. In contrast, if there are many fault planes and striation data available, but the interpretation of the displacement sense is difficult, one should use the method of WALLBRECHER & FRITZ because it needs only a few displacement sense indicators. If there is need to quantify the stress ellipsoid explicitely (shape factor) one would use the method of WALLBRECHER & FRITZ. In most cases it is sufficient to determine the deformation symmetry qualitatively to answer geological questions; so that SCHRADER's method could be preferred.

The orientation tensor method (WALLBRECHER & FRITZ, 1989) is an automatised system without the possibility to interprete individual fault plane data. There are tools to test the reliability of the results but there is, until now, no possibility to separate superimposed deformations. SCHRADER's method allows the recognition of superimposed deformation processes and the analysis of each of them. Thus the best way is to use both methods.

The geological meaning of the results can only be understood in the context of the whole deformation structure. The texture of at least one complete fold or thrust unit (SCHRADER, in press) must be examined, especially the relationship of faults to bedding to assign faulting to pre-, syn- or postkinematic processes.

Acknowledgements

We thank W. UNZOG (Graz) for many hours of discussion and the considerable work on the computer programs and F. NEUBAUER (Graz) who reviewed a prior version of this paper.

Literatur

ALEKSANDROWSKI, P.: Graphical determination of principal stress directions for slickenside lineation populations: an attempt to modify Arthaud's method. – J. Struct. Geol., **7** , 73–82, 1985.

ANDERSON, E. M.: The dynamics of faulting. – Oliver & Boyd, Edinburgh, 1952.

ANGELIER, J. & GOGUEL, J.: Sur une méthode simple de détermination des axes principaux des contraintes pour une population de failles. – C. R. hebd. Séanc. Acad. Sci. Paris, **288**, 307–310, 1979.

ANGELIER, J. & MANOUSIS, S.: Classification automatique et distinction des phases superposées en tectonique de failles. – C. R. hebd. Séanc. Acad. Paris, **290**, 651–654, 1980.

ANGELIER, J. & MECHLER, P.: Sur une méthode graphique de recherche des contraintes principales également utilisable en tectonique et en séismologie: la méthode des dièdres droits. – Bull. Soc. géol. France, **19**, 1309–1318, 1977.

ARMIJO, R., CAREY, E. & CISTERNAS, A.: The inverse problem in microtectonics and the seperation of tectonic phases. – Tectonophysics, **82**, 145–160, 1982.

ARMIJO, R. & CISTERNAS, A.: Un problème inverse en microtectonique cassante. – C. R. hebd. Séanc. Acad. Paris, **287**, 595–598, 1978.

ARTHAUD, F.: Méthode de détermination graphique des directions de raccourcissement, d'allongement et intermédiare d'une population de failles. – Bull. Soc. géol. France, **7/11**, 729– 737, 1969.

BEMMELEN VAN, R.W.: Beitrag zu Geologie der Gailtaler Alpen (Kärnten, Österreich), zweiter Teil. Die zentralen Gailtaler Alpen. – Jb. Geol. B.-A., **104**, 213–237, 1961.

BOTT, M. H..P.: The mechanics of oblique slip faulting. – Geol. Mag., **96**, 109–117, 1959.

CAREY, E.: Analyse numérique d'un modèle mecanique élémentaire appliqué à l'étude d'une population de failles: calculation d'un tenseur moyen des contraintes à partir de stries de glissement. – Thèse 3eme cycle, Université de Paris-Sud, 1976.

CAREY, E.: Recherche des directions principales de contraintes asociées au jeu d'une population de failles. – Rév. Géol. dyn. Géophys., **21**, 57–66, 1979.

CAREY, E. & BRUNIER, B.: Analyse théorique et numérique d'une population de failles. – C. R. hebd. Séanc. Acad. Paris, **279**, 891–894, 1974.

DE VICENTE, G.: The e/k' Diagram. An application of the "slip model" to the populational fault analyses. – Rev. Soc. Geol. España, **1**, 97–112, 1988.

ETCHECOPAR, A., VASSEUR, G. & DAIGNIERES, M.: An inverse problem in microtectonics for the determination of stress tensors from fault striation analyses. – J. Struct. Geol., **31**, 51–65, 1981.

HEINISCH, H.: Concepts for the geological evolution of Gailtal crystalline (Kärnten, Austria). – In: FLÜGEL, H. W., SASSI, F. P. & GRECULA, P. (eds.): Pre-Variscan and Variscan events in the Alpine-Mediterranean mountain belts, 295–312, Alfa Publisher, Bratislava 1988.

HEINISCH, H., SCHMIDT, K. & SCHUH, H.: Zur geologischen Geschichte des Gailtalkristallins im unteren Lesachtal westlich von Kötschach-Mauthen (Kärnten, Österreich). – Jb. Geol. B.-A., **126**, 447–486, 1984.

HOEPPENER, R.: Tektonik im Schiefergebirge. – Geol. Rdsch., **44**, 22–58, 1955.

HOEPPENER, R.: Zur physikalischen Tektonik. Darstellung der affinen Deformationen, der Spannungs- und Beanspruchungszustände mit Hilfe der flächentreuen Kugelprojektion. – Felsmech. Ing.-Geol., **2**, 22–44, 1964.

KARMAN, T. von: Festigkeitsversuche unter allseitigem Druck. – Zeitschr. Ver. dt. Ingenieure, **55**, 1749–1957, 1911.

MANDL, G.: Mechanics of tectonic faulting; models and basic concepts. – 407p., Elsevier, Amsterdam 1988.

NORRIS, D.K. & BARRON, K.: Structural analyses of features on natural and artificial faults. – GSC Paper, **68/52**, 135–174, 1968.

PFIFFNER, O.A. & BURKHARD, M.S.: Determination of paleostress axes orientations from fault, twin and earthquake data. – Annales Tectonicae, **1**, 48–57, 1987.

PRICE, N.J.: Fault and joint development in brittle and semibrittle rocks. – 176p., Pergamon Press, 1966.

RAMBERG, H.: Particle path, displacement and progressive strain applicable to rocks. – Tectonophysics, **28**, 1–37, 1975.

SCHÖNLAUB, H.P.: Das Paläozoikum in Österreich. Verbreitung, Stratigraphie, Korrelation, Entwicklung und Paläogeographie nichtmetamorpher und metamorpher Abfolgen. – Abh. Geol. B.-A. Wien, **33**, 124p., 1976.

SCHÖNLAUB, H.P.: Geologische Karte der Republik Österreich, Blatt ÖK 179 Kötschach, 1 : 50.000. – Geol. B.-A. Wien, 1985.

SCHÖNLAUB, H.P.: Geologische Karte der Republik Österreich, Blatt ÖK 178 Weissbriach, 1 : 50.000. – Geol. B.-A. Wien, 1987.

SCHRADER, F.: Graphische Methode der Strain- und Streßanalyse von Scherkluftgesellschaften. – Nachr. dt. Geol. Ges., **37**, 53– 54, 1987.

SCHRADER, F.: Das regionale Gefüge der Drucklösungsdeformation an Geröllen im westlichen Molassebecken. – Geol. Rdsch., **77**/2, 347–369, 1988a.

SCHRADER, F.: Das Verschiebungsfeld von Spalten, Harnischen und Stylolithen. – Symposium Tektonik – Strukturgeologie – Kristallingeologie (TSK II), Abstract, 95–96, Erlangen, 1988b.

SCHRADER, F.: Symmetry of pebble-deformation involving solution pits and slip-lineations in the northern Alpine Molasse Basin. – J. Struct. Geol., **10**/1, 41–52, 1988c.

SCHRADER, F.: Analyse von Bewegungsspuren auf Harnischen in Falten des Ahrtals (Rheinisches Schiefergebirge). – In press.

SIMON GOMES, J. L.: Analyses from a gradual change in stress regimes (example from the Eastern Iberian Chain, Spain) . – Tectonophysics, **124**, 37–53, 1986.

UNZOG, W.: Schertektonik im Gailtalkristallin und am Südrand des Drauzuges (Kärnten, Österreich). – Symposium Tektonik – Strukturgeologie – Kristallingeologie (TSK II), Abstract, 125– 126, Erlangen, 1988.

UNZOG, W.: Schertektonik im Gailtalkristallin und an seiner Begrenzung. – Unveröff. Diss. Univ. Graz, 204 p., Graz, 1989.

UNZOG, W.: Paläostress am Drauzugsüdrand. – Symposium Tektonik – Strukturgeologie – Kristallingeologie (TSK III), Abstract, 261–264, Graz 1990.

WALLBRECHER, E.: Tektonische und gefügeanalytische Arbeitsweisen. – 224p., Enke, Stuttgart, 1986.

WALLBRECHER, E. & FRITZ, H.: Eine Methode zur quantitativen Erfassung von Gestalt und Orientierung des Stress-Ellipsoids aus Harnischflächen und Striemungen. – 2. Symposium Tektonik – Strukturgeologie – Kristallingeologie (TSK II), Abstract, 131–132, Erlangen, 1988.

WALLBRECHER, E. & FRITZ, H.: Quantitative evaluation of the shape factor and the orientation of a paleo-stress ellipsoid from the distribution of slickenside striations. – Annales Tectonicae, **3**/2, 110–122, 1989.

Manuskript bei der Schriftleitung eingelangt am 30. April 1990.